

# Crosstalk Analysis of Multiwavelength Optical Cross Connects

Tim Gyselings, *Student Member, IEEE*, Geert Morthier, *Member, IEEE, Member, OSA*,  
and Roel Baets, *Senior Member, IEEE, Member, OSA*

**Abstract**—This paper presents the results of a crosstalk analysis of four optical wavelength division multiplexed (WDM) cross-connect (OXC) topologies. An optimal set of parameters is determined to reduce the total crosstalk. The scalability of the topologies is presented in terms of wavelengths and input fibers. The total crosstalk in function of the number of cascaded OXC's is compared for the four topologies.

**Index Terms**—Optical communication, optical crosstalk, optical cross connect (OXC), optical switches, optical wavelength conversion, wavelength division multiplexing (WDM).

## I. INTRODUCTION

OPTICAL wavelength division multiplexing (WDM) networks are very promising due to their large bandwidth, their large flexibility and the possibility to upgrade the existing optical fiber networks to WDM networks [1]–[8]. WDM has already been introduced in commercial systems. All-optical cross connects (OXC), however, have not yet been used for the routing of the signals in any of these commercial systems. Several OXC topologies have been presented in the literature, but their use has so far been limited to field trials, usually with a small number of input–output fibers and/or wavelength channels [9]–[20], [27]–[36]. The fact, that in practical systems many signals and wavelength channels could influence each other and cause significant crosstalk in the optical cross connect, has probably prevented the use of OXC's in commercial systems [21]–[23], [26], [31], [41], [42].

The crosstalk levels in OXC configurations presented so far are generally so high that they give rise to a significant signal degradation and to an increased bit error probability. Because of the complexity of an OXC, different sources of crosstalk exist, which makes it difficult to optimize the component parameters for minimum total crosstalk. In this paper, the crosstalk of four different OXC topologies is calculated and compared with each other, and the influence of the component crosstalk on the total crosstalk is identified.

We present an analytical approximation for the total crosstalk level of four different OXC topologies, which makes the component parameter optimization considerably easier.

Manuscript received May 15, 1998; revised March 22, 1999. This work was supported in part by the European ACTS Project OPEN (AC066) and the European ACTS Project PHOTON (AC0084). The work of T. Gyselings was supported by the Flemish Institute for Science and Technology (IWT).

The authors are with the Department of Information Technology, University of Gent, IMEC, Sint-Pietersnieuwstraat 41, B-9000 Gent, Belgium (e-mail: tim.gyselings@intec.rug.ac.be).

Publisher Item Identifier S 0733-8724(99)06342-2.

The crosstalk sources are related to the different individual components of the OXC's.

This paper is divided into four main parts. In the first part the different OXC topologies are presented and explained. The different crosstalk sources in the OXC are identified and quantified in the second part. Afterwards the analytical equations for the topologies are derived. The results are presented in part four. The analytical approach is validated by comparing the results obtained by the analytical equation with results obtained by numerical simulations. Afterwards the influence of the component parameters on the crosstalk is studied. In the next paragraph the scalability in terms of number of wavelengths and number of input/output fibers, is investigated. Finally the crosstalk levels of the four topologies are compared in function of the number of cascaded OXC's.

## II. OXC TOPOLOGY

Several topologies exist for all optical WDM cross connects. The most suitable topology for an application depends in general on the required functionality and on the cost, capacity and flexibility constraints. In this paper, we evaluate the influence of two switching matrices and the use of wavelength converters on the crosstalk properties of an OXC. The impact on the crosstalk when swapping the order between switching and selecting (of the wavelength channel) has been studied. That is why different OXC topologies have been defined and the crosstalk of each of these has been evaluated. By comparing the results of the different topologies one can derive the influence of the switching matrix, of the wavelength converters and of the order between switching and selecting. The topologies defined in this paper are not the only possible, but are generic topologies that make it possible to evaluate the crosstalk properties.

The first switching matrix that was studied is based on an array of gates. The first OXC topology includes this switching matrix to route the different wavelength channels. Splitters and combiners are placed in front of and behind the switch matrix and filters are used to select the wavelength channels. The broadcast and select optical cross connect topology is shown in Fig. 1 [10], [11], [14], [15].

Another switching matrix studied in this paper is based on a mechano-optical space switch. This switching matrix is embedded in an OXC topology (Fig. 2) that makes use of demultiplexers and multiplexers to select the wavelength channels.

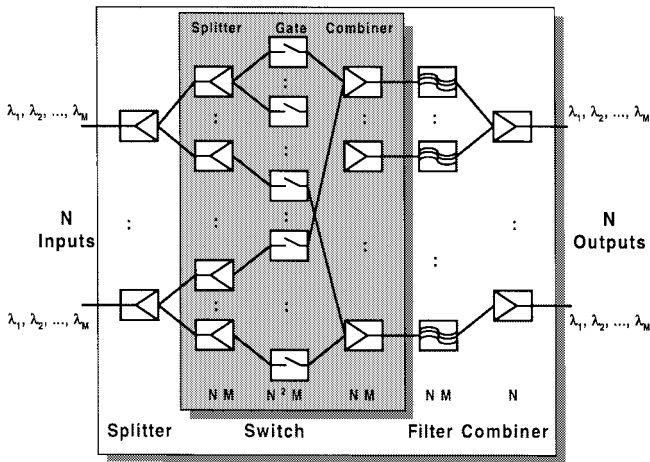


Fig. 1. Topology 1: OXC switch based on gates.

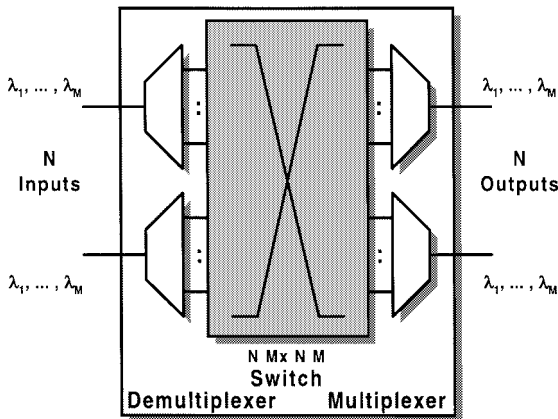


Fig. 2. Topology 2: OXC switch based on space switch.

To analyze the impact when swapping the order between switching and selecting of the wavelength channels, a third OXC topology has been defined (Fig. 3). This topology is the mirror image of the first one. The switching matrix of topology 1 is used but the wavelength channels are selected by the filters, before being routed to the desired output fiber.

The effect of wavelength converters on the signal quality has been investigated by adding converters to the first topology (Fig. 4). Wavelength converters are often desired in the OXC to make the network management much easier, to reduce the blocking probability and because of their signal regeneration and noise reduction capabilities [49], [50], [53]. The drawback of the wavelength converter is the price and the higher complexity of the system. I would like to stress that only this topology needs tuneable filters. The filters used in the first and the third topology have a fixed centre frequency.

#### A. Principal of the Topologies

In the first topology (Fig. 1) the wavelength channels are first routed to the desired output fiber before being selected by a filter. The  $N$  input fibers are routed to the desired  $N$  output fibers, each carrying  $M$  wavelength channels. A  $NM \times NM$  space switch is used to route a signal to the desired output fiber. This switch consists of passive splitters ( $N \times M$ ), gates ( $N^2 \times M$ ) and combiners ( $N \times M$ ).

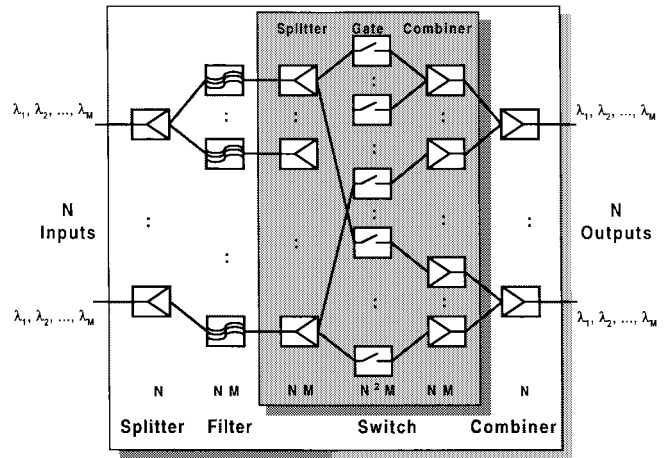


Fig. 3. Topology 3: OXC switch based on gates, the wavelength channel is selected before switched.

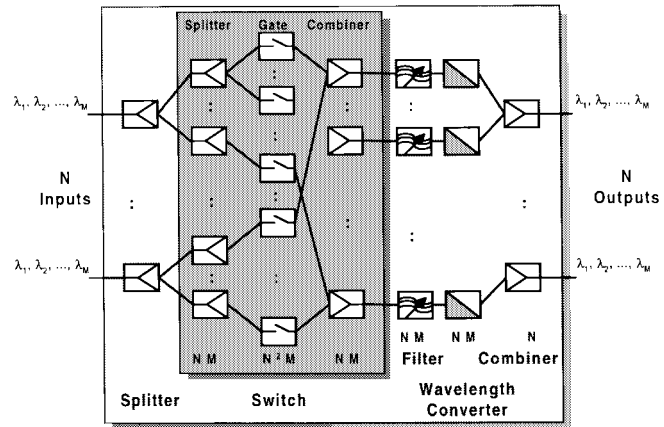


Fig. 4. Topology 4: OXC switch based on gates, wavelength converters are included after the switch.

The gates are implemented as gain-clamped semiconductor optical amplifiers (GC-SOA) [25]. After this switching part, the correct wavelength is selected by a filter with a fixed centre frequency. Finally,  $N$  times  $M$  outputs with a different central wavelength, are combined into the  $N$  output fibers.

In the second topology (Fig. 2) the  $N$  input fibers are demultiplexed by  $N$  demultiplexers. A  $NM \times NM$  space switch routes the channels to the output fibers. This space switch can be implemented as a mechano-optical space switch.  $N$  times  $M$  channels are combined by  $N$  multiplexers. The multiplexers and demultiplexers can be implemented for example as phased arrays [23].

The third topology (Fig. 3) acts more or less the same as the first one. The difference is that the desired wavelength channel is selected by the filter (with a fixed centre frequency) before the channel is routed to the output fiber.

In the last topology (Fig. 4) the wavelength channel is converted to another (or the same) wavelength by a wavelength converter which is assumed to be a Mach-Zehnder interferometric wavelength converter in contra directional mode [24], [51]. This converter is placed behind the filter, which has to be tuneable. Finally,  $N$  times  $M$  outputs with a different central wavelength, are combined into the  $N$  output fibers.

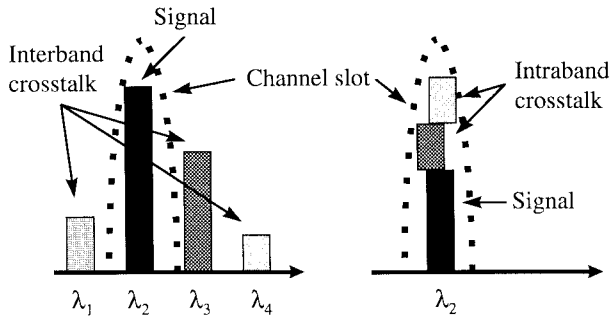


Fig. 5. Interband and intraband crosstalk.

### III. CROSSTALK SOURCES

Crosstalk will be one of the major limitations for the introduction of OXC in all optical networks. In this paper the influence of the components on the total OXC crosstalk is investigated. The different classes of crosstalk are first clarified.

Different kinds of crosstalk exist, depending on their source. First one has to make a distinction between interband crosstalk and intraband crosstalk [27], [39], [42]. Interband crosstalk is the crosstalk situated in wavelengths outside the channel slot (Fig. 5) (wavelengths outside the optical bandwidth). This crosstalk can be removed with narrow-band filters and it produces no beating during detection, so it is less harmful. The crosstalk within the same wavelength slot is called intraband crosstalk. It cannot be removed by an optical filter and therefore accumulates through the network. Since it cannot be removed, one has to prevent the crosstalk. In this paper intraband crosstalk is studied since the network performance will be limited by this kind of crosstalk. Moreover, within the intraband crosstalk, a distinction between incoherent and coherent crosstalk has to be made. These types of crosstalk are not well defined in literature and therefore a definition is given here. To make a distinction between both types of intraband crosstalk one has to look at the consequences. The interference of the signal channel and the crosstalk channel at the detector results in a beat term. The crosstalk is called coherent crosstalk if the total crosstalk is dominated by this beat. If this beat term is very small compared with the total crosstalk, it is called incoherent. This difference will be illustrated hereafter.

The output power of a combiner and a detector with two inputs is given in (1) (Fig. 6)

$$P_{\text{out}} = P_1 + P_2 + 2\sqrt{P_1 P_2} \cos[(\omega_1 - \omega_2)t + \Phi_1(t) - \Phi_2(t) + \Theta_1 - \Theta_2] \quad (1)$$

with  $P_1$  and  $P_2$  the power of both signals,  $\omega_1$  and  $\omega_2$  the pulsation,  $\phi_1(t)$  and  $\phi_2(t)$  the phase of the signals in function of the time and  $\Theta_1$  and  $\Theta_2$  the initial phase of both signals.

This output power is composed of three terms. The first term is the power of the first input channel. The second term is the power of the second input channel. In a normal optical network the power of this channel will be much lower. The third term is the beat term between the two input channels. The power of this beat term depends on the root of the powers (if the second power is  $X$  times lower than the first one, the beat term is only  $\sqrt{X}$  lower!). Furthermore this beat term

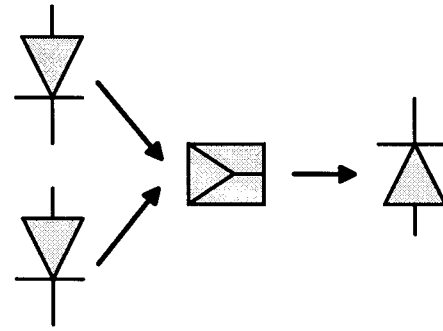


Fig. 6. Crosstalk sources.

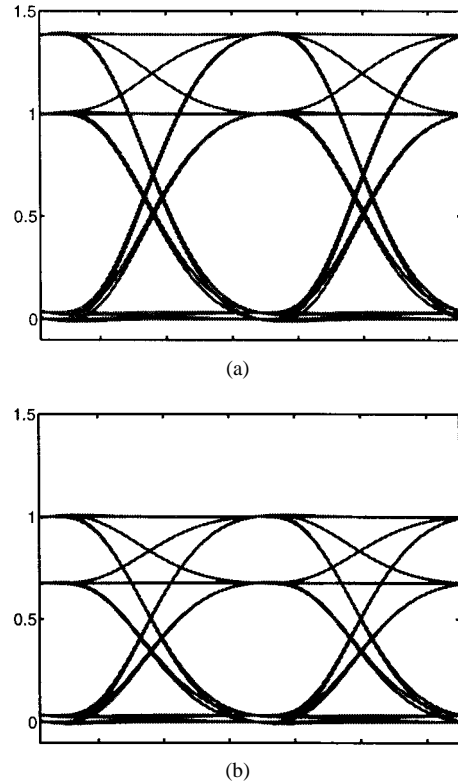


Fig. 7. Eye diagram for positive (a) and negative (b) sign, for a crosstalk value of  $-15$  dB.

depends on the frequency difference between both channels, on the phase difference in function of the time and on the initial phase difference of both channels by way of a cosine function [23], [26], [27], [37], [38], [40], [43]–[45]. Incoherent crosstalk is defined as the case in which the beat term can be neglected (e.g., when the wavelengths are different). The case in which the beat term cannot be neglected is called coherent crosstalk. This crosstalk occurs in a WDM network if channels with the same nominal carrier frequency are combined. The power of the beat term varies in time, but has a maximum value of  $\pm 2\sqrt{P_1 P_2}$ . Notice that the beat term can be positive or negative. The decrease in eye opening strongly depends on the sign of the beat term. A positive sign does not affect the eye opening, a negative sign results in a decrease. In Fig. 7 the eye is shown for both signs, when the frequency and phase difference is zero ( $P_2$  is 15 dB lower than  $P_1$ ). Since this sign cannot be predicted in a system it should be designed for the

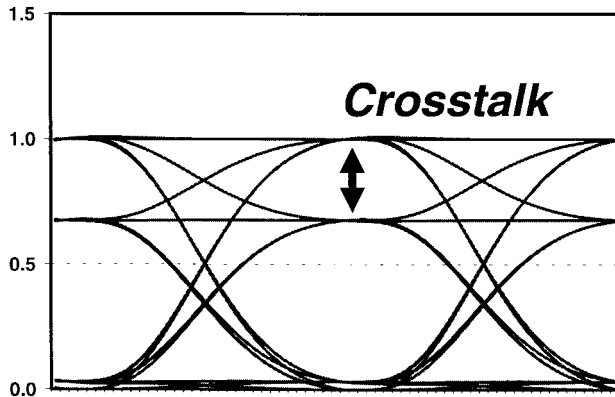


Fig. 8. Definition of crosstalk.

worst case, which is the negative sign. If coherent crosstalk is considered in this paper we will assume a maximal negative beat.

From the eye diagrams shown in the figures one can conclude that interferent crosstalk is much more harmful for the “one” than for the “zero.” In this paper, the calculated crosstalk is defined as the difference between a calculation without crosstalk sources and a calculation with crosstalk sources, for all “ones” at the input. In the case of coherent crosstalk all the beat terms have the same sign, resulting in a worst case situation. Summarized the calculated crosstalk is the difference between a “one” without crosstalk and a “one” with crosstalk. This is illustrated in Fig. 8.

We will now identify the crosstalk sources of the topologies considered in this paper. The different crosstalk sources in the topology of Fig. 1 are the following. The gate adds crosstalk due to nonperfect gain clamping in the amplifier; the gain dynamics of the GC-SOA depend on the total input power [25], [47]. The output of the gate can be modeled as  $P_{\text{out}} = P_{\text{in}} + P_{\text{cros}}$  if the amplification by the gate is neglected. The crosstalk power at wavelength  $i$  is then given by (by definition of  $X_{\text{gate}}$ )

$$P_{\text{cros},i} = X_{\text{gate}} P_{\text{in},i} \sum_{k=1}^M P_{\text{in},k} \quad (2)$$

with  $X_{\text{gate}}$  the crosstalk parameter of the GC-SOA,  $P_{\text{in},k}$  the power at wavelength  $k$  and  $M$  the number of wavelength channels at the input of the gate. The sum is made over all  $M$  wavelength channels.

At the combiner after the gates,  $N$  signals are combined coming from different input fibers. During normal operation one of the  $N$  gates is in the on-state and all the other are in the off-state. Because of the nonperfect blocking of the gates in the off-state some of the power is leaking through the gate. That effect also results in crosstalk.

The combiner at the output of the OXC has  $M$  inputs. Each of these inputs consists of one signal channel and  $M - 1$  suppressed channels (suppressed by the filter). This means that each output channel of the combiner has  $M$  contributions, one signal contribution and  $M - 1$  suppressed channels. This leads to crosstalk.

In the OXC of Fig. 2 crosstalk is added in the space switch and in the multiplexer. The output of the space switch contains contributions of all inputs. Since only one of the inputs contains the signal, all other contributions should be considered as crosstalk (they will be attenuated by the switch). A multiplexer acts as a filter and a combiner which means that the  $M$  inputs of the multiplexer carry each  $M$  channels [52].  $M - 1$  of these channels are suppressed by the filter effect of the multiplexer. Therefore, one output channel is composed of  $M$  contributions, one signal input channel and  $M - 1$  suppressed input channels.

The same crosstalk sources of topology 1 can be identified in the topology of Fig. 3. The difference is that at the input of each gate  $M - 1$  of the  $M$  channels are suppressed by the filter, resulting in less crosstalk due to the nonperfect gain clamping of the gate.

In Fig. 4, there is a wavelength converter between the filter and the combiner. The input of an additional wavelength converter consists of one channel carrying the signal under study and  $M - 1$  suppressed channels. This leads to crosstalk because the output of the wavelength converter depends on the total input power (but the converter has also some regeneration effect). At the output of the wavelength converter there is only one channel. (The wavelength converter is used in contra directional mode [24], [51]. Due to this effect, the combiner at the end of the OXC adds no crosstalk because the  $M$  input fibers of the combiner carry only one channel, each with a different wavelength.

#### IV. ANALYTICAL EXPRESSION FOR THE CROSSTALK

In this paragraph, analytical expressions are given that describe the output power of a certain OXC topology in function of the input powers and component parameters. Note that absolute power levels are only relevant in front of the GC-SOA. Therefore the power levels at the input of the gate are taken as reference, gains and losses are not relevant since they are assumed uniform for all possible routing ways. The crosstalk is determined by calculating the difference in output power between a calculation without crosstalk (one channel at the input) and a calculation with crosstalk (all possible channels at the input) (maximal crosstalk, so full traffic load is assumed). The calculations are performed for only “ones” at the input. The sign of the beat terms is assumed negative and the amplitude of the beat terms is assumed maximum to calculate worst case conditions.

The crosstalk is calculated for a certain wavelength channel; this channel will be called the channel under study. The analytical equations for the OXC topologies are illustrated in this paragraph. In the equations the signal power is defined by  $P_i^j$ , where  $i$  designates the wavelength channel and  $j$  the number of the fiber. The fiber which contains the channel under study is indicated  $j_0$ , the wavelength under study  $i_0$ . If a wavelength converter is used, the wavelength under study at the output is redefined  $i_0$ .  $M$  is the number of wavelength channels in a fiber and  $N$  is the number of input fibers.

The ON-OFF ratio of the gate is given by  $R_{\text{gate}}^{-1}$ , so that  $R_{\text{gate}}$  is the transmission of a gate in the off-state ( $< 1$ ).  $X_{\text{gate}}$

is the crosstalk parameter of the gate, defined in (2). The suppression of a wavelength channel by a filter is given by  $T_F^{-1}$ . This means that  $T_F$  is the transmission of the filter seen by that channel ( $<1$ ). The crosstalk of the switch matrix is given by  $X_{sw}$  and is defined as the fraction of the input power routed to other outputs. The crosstalk of the demultiplexer and the multiplexer are given by  $X_{demux}$  and  $X_{mux}$  and are also defined as transmission factors ( $<1$ ).

Equation (3), shown at the bottom of the page, is given for the first topology in case of coherent crosstalk. The first three terms are the noninterfering contributions, the last three terms are the contributions due to the interference of different channels (beat terms).

The first term contains the input power. The output power would be equal to the input power if no interaction with the other channels existed. The second term contains the crosstalk of the gate due to nonperfect gain clamping. The third term contains contributions due to input channels with the same wavelength at other input fibers. These are the direct crosstalk contributions, resulting in an increase of the output power. The interference between the channels results in the last three terms, with the negative sign. First there is the interference between the signal channel and the crosstalk channels. Notice that these contributions only scale with the root of  $R_{gate}$  and  $T_F$  resulting in severe signal degradation. The second interference term contains the beat terms of the different crosstalk channels. Since each of these crosstalk channels is composed of different contributions (e.g.,  $N - 1$  times the contribution  $PR_{gate}$ ), beat terms between these contributions have to be taken into account (last term).

The equation for the second topology differs from the previous one because other components are used (space switch and multiplexers–demultiplexers). A simplified version of the equation is given below with only the most dominant contributions shown in (4) at the bottom of the page. The results shown in this paper are based on a full equation. Five contributions can

be distinguished. The first term is the input signal. The second term contains the direct crosstalk contributions. The beat terms are given in the next three terms. First, we have the interference between the  $N - 1$  crosstalk contributions. Afterwards, the beat between signal and crosstalk channels is given. The last term is the beat between different crosstalk contributions.

The equation for the third topology, shown in (5) at the bottom of the next page, is rather equal to the equation for the first topology. The same six contributions can be distinguished. The only difference between both equations (and OXC) is that the crosstalk due to the not-perfect gain clamping of the gate is less important in this topology because the other wavelength channels are filtered before the gate. The other contributions are the same.

The equation of the fourth topology is more difficult due to the nonlinear behavior of the wavelength converter. The input-output characteristic of the wavelength converter is modeled by an analytical function which agrees very well with simulation results of a Mach–Zehnder Interferometric (MZI) wavelength converter (Fig. 9) [46], [51]. The numerical model used for the simulation is based on [48]. The output of the converter is given by

$$P_{out} = f(P_{in}) = a \tanh\left(b\left(P_{in} - \frac{1}{2}\right)\right) + \frac{1}{2}$$

The parameters  $a$  and  $b$  are determined by

$$f(0) = 0$$

and

$$f'\left(\frac{1}{2}\right) = 2$$

with  $P_{in}$  and  $P_{out}$  normalized between zero and one.

The equation for the total OXC is a mixture of the equation for the first topology and this analytical function. The signal before the combiner at the output of the OXC is used as input

$$\begin{aligned} P_{i_0}^{out} = & P_{i_0}^{j_0} + P_{i_0}^{j_0} \left\{ X_{gate} \left( (M-1)P_{i_0}^{j_0} + P_{i_0}^{j_0} \right) \right\} \\ & + P_{i_0}^j \left\{ \begin{array}{l} (N-1)R_{gate} [1 + X_{gate} M P_{i_0}^j] \\ + (M-1)T_F [1 + X_{gate} M P_{i_0}^j] \\ + (M-1)(N-1)T_F R_{gate} \end{array} \right\} - 2\sqrt{P_{i_0}^{j_0}} \sqrt{P_{i_0}^j} \left\{ \begin{array}{l} (N-1)\sqrt{R_{gate}} \\ + (M-1)\sqrt{T_F} \\ + (N-1)(M-1)\sqrt{R_{gate}T_F} \end{array} \right\} \\ & - 2P_{i_0}^j \left\{ \begin{array}{l} (N-1)(M-1)\sqrt{R_{gate}T_F} \\ + (N-1)^2(M-1)R_{gate}\sqrt{T_F} \\ + (N-1)(M-1)^2\sqrt{R_{gate}T_F} \end{array} \right\} - 2P_{i_0}^j \left\{ R_{gate} \sum_{t=1}^{N-2} t + T_F \sum_{t=1}^{M-2} t + R_{gate}T_F \sum_{t=1}^{(M-1)(N-1)-1} t \right\}. \quad (3) \end{aligned}$$

$$\begin{aligned} P_{i_0}^{out} = & P_{i_0}^{j_0} + P_{i_0}^j [X_{sw}(N-1)] - 2P_{i_0}^j \left[ X_{sw} \sum_{t=1}^{N-2} t \right] - 2\sqrt{P_{i_0}^{j_0}} \sqrt{P_{i_0}^j} \\ & \times \left[ \begin{array}{l} \sqrt{X_{sw}X_{demux}}N(M-1) + \sqrt{X_{sw}}(N-1) \\ + \sqrt{X_{mux}X_{sw}}(M-1)N + \sqrt{X_{mux}X_{demux}}(M-1) \\ + \sqrt{X_{mux}X_{sw}X_{demux}}(M-1)(NM-N-1) \end{array} \right] - 2P_{i_0}^j \left[ \begin{array}{l} X_{sw}\sqrt{X_{demux}}N(N-1)(M-1) \\ + X_{sw}\sqrt{X_{mux}}N(N-1)(M-1) \\ + \sqrt{X_{mux}X_{sw}X_{demux}}(M-1)(N-1) \end{array} \right]. \quad (4) \end{aligned}$$

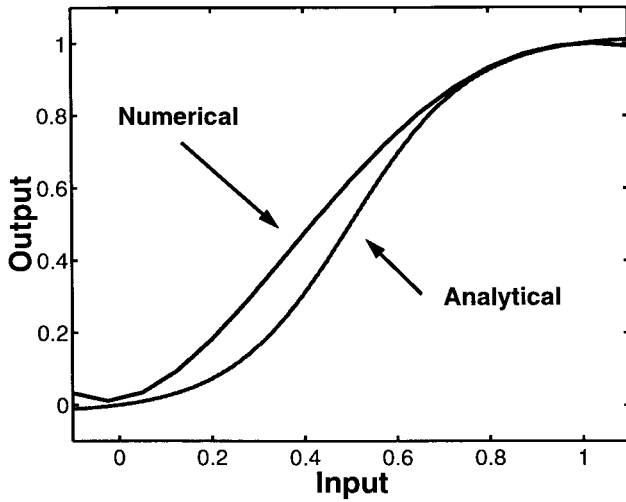


Fig. 9. Analytical function compared with a numerically simulated wave-length converter input-output function.

for the analytical function and the outputs of this function are combined to form the output of the OXC.

### V. NUMERICAL RESULTS

The parameter values used for the calculations are given in Table I, except when stated otherwise. The calculated crosstalk is defined as

$$\text{Crosstalk} = \frac{P_{\text{out}}^{\text{all channels}} - P_{\text{out}}^{\text{reference}}}{P_{\text{out}}^{\text{reference}}} \quad (6)$$

with  $P_{\text{out}}^{\text{all channels}}$  the output power of a calculation with all channels at the input and  $P_{\text{out}}^{\text{reference}}$  the output power of a calculation with only the channel under study at the input of the OXC.

The input power is chosen to be very low. As mentioned before, power levels at the input of the gate are taken as reference. A power value of  $-20$  dBm is a normal input value for a gate.

#### A. Validation of the Analytical Approach

The analytical approach has been validated by calculating the crosstalk for the first OXC topology as a function of the input power and comparing this result with the results of a numerical simulation of the same topology.

The numerical simulations are performed in the time domain. The concept of the simulation tool is that each compo-

TABLE I  
PARAMETER VALUES USED FOR THE CALCULATIONS

$R_{\text{gate}}$	- 50 dB
$X_{\text{gate}}$	- 0.1 mW <sup>-1</sup>
$T_F$	- 30 dB
P input	- 20 dBm
$X_{\text{mux}}$	- 30 dB
$X_{\text{demux}}$	- 30 dB
$X_{\text{switch}}$	- 60 dB
M	4
N	2

nent is represented by a function which calculates the optical fields at the output of the component based on the optical fields at the input and on the component parameters. The system model of the gate used in these simulations is controlled by comparing with results obtained by a detailed numerical simulation described in [47]. The filter is implemented as a Fabry-Perot filter, with a free spectral range of 70 nm (larger than twice the used bandwidth). The channel spacing is 3.2 nm and four channels are used. The parameter  $T_F$  given in Table I is defined as the transmission factor seen by the neighboring channel. Wavelengths further from the central wavelength of the filter are suppressed more. Therefore we expect higher analytical crosstalk than numerical crosstalk because in the numerical simulations the suppression of non-adjacent channels is higher. In the case presented in this paper there was one nonadjacent channel (four wavelengths were used and the crosstalk was calculated at one of the centre wavelengths).

The results of the analytical calculation and the numerical simulation are shown in Fig. 10. In this paragraph, the difference between the analytical calculations and the numerical simulations is discussed. The shape of the figure is discussed

$$\begin{aligned}
 P_{i_0}^{\text{out}} = & P_{i_0}^{j_0} + P_{i_0}^{j_0} \left\{ X_{\text{gate}} \left( (M-1) T_F P_i^{j_0} + P_{i_0}^{j_0} \right) \right\} \\
 & + P_{i_0}^j \left[ \frac{(N-1) R_{\text{gate}} \left[ 1 + X_{\text{gate}} M T_F P_i^j \right]}{+(M-1) T_F \left[ 1 + X_{\text{gate}} M T_F P_i^j \right]} \right] - 2 \sqrt{P_{i_0}^{j_0}} \sqrt{P_{i_0}^j} \left\{ \frac{(N-1) \sqrt{R_{\text{gate}}} + (M-1) \sqrt{T_F}}{+(N-1)(M-1) \sqrt{R_{\text{gate}} T_F}} \right\} \\
 & - 2 P_{i_0}^j \left\{ \frac{(N-1)(M-1) \sqrt{R_{\text{gate}} T_F}}{+(N-1)(M-1)^2 \sqrt{R_{\text{gate}} T_F}} \right\} - 2 P_{i_0}^j \left\{ R_{\text{gate}} \sum_{t=1}^{N-2} t + T_F \sum_{t=1}^{M-2} t + R_{\text{gate}} T_F \sum_{t=1}^{(M-1)(N-1)-1} t \right\}. \quad (5)
 \end{aligned}$$

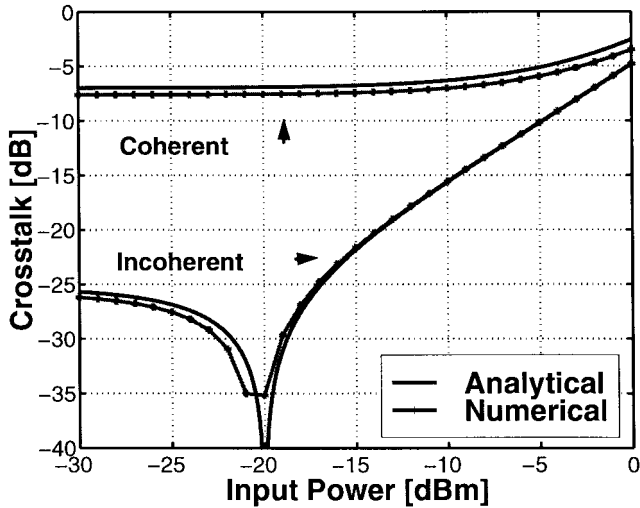


Fig. 10. Topology 1: Crosstalk versus input power for four wavelength channels.

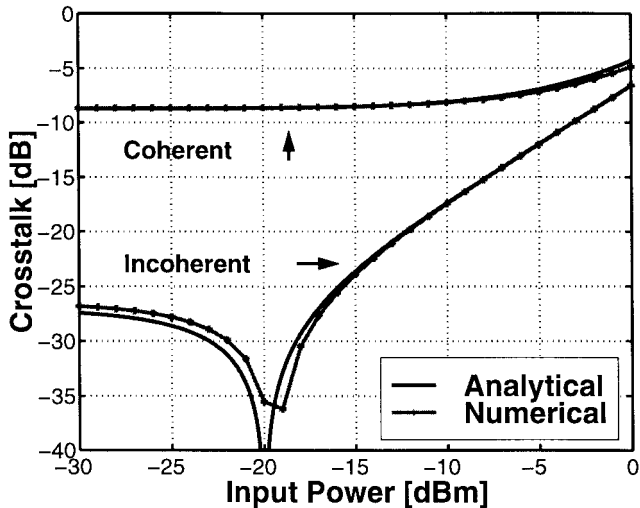


Fig. 11. Topology 1: Crosstalk versus input power for three wavelength channels. The crosstalk is calculated for the center wavelength.

in Section V-B. The two lines at the bottom of Fig. 10 give the incoherent crosstalk. The two lines at the top are for the coherent case. The crossed lines are the simulated results, the straight lines the analytical results.

It can be seen that, as expected, the crosstalk predicted by the analytical equation is higher than the one obtained from simulations. This is due to the filter effect. To eliminate this effect the crosstalk is also calculated in the case of three wavelengths. The crosstalk is calculated at the central wavelength, both adjacent wavelengths have the same suppression (analytically and numerically). The results are shown in Fig. 11. There is still a small difference between the analytical result and the simulation result. This is due to the fact that the analytical equation is still an approximation. Not all possible terms are taken into account to keep the equation relatively simple. Nevertheless, good agreement between numerical simulations and analytical calculations is shown. Analytical calculations have the advantage that they give a better insight in the influence of a certain component on the

total performance and the calculations are much faster than the numerical simulations. The drawback is that only static results are derived.

### B. Influence of Component Parameters

The influence of the component parameters and the input power on the total crosstalk is calculated. The aim of these calculations is to optimize the parameter values for the OXC and to identify the most critical components.

1) *Input Power*: This parameter is only relevant for the topologies with a switch based on gates. The crosstalk as a function of the input power has already been shown in Fig. 10, for the first topology. The first conclusion which can be drawn from this figure is that there is a big difference between coherent and incoherent crosstalk, both in value and shape. Some of the interfering terms in the analytical equation (3) are only reduced by a factor  $\sqrt{T_F}$  and they give rise to high-coherent crosstalk. This coherent crosstalk is due to interference of channels from different input fibers and can strongly be reduced if the conditions for coherent crosstalk are not fulfilled. Nevertheless, due to the good alignment of the laser sources in a WDM network, it is likely that different channels interfere coherently. In the next figures only coherent crosstalk is shown.

The second conclusion is that there is a difference in shape between the coherent and incoherent case. In the coherent case the crosstalk increases slightly with increasing input power. In the incoherent case, the crosstalk has a dip for a certain power and increases when the power is increased. This effect is caused by the crosstalk of the GC-SOA used as gate. The higher the input power of the gate, the more crosstalk is added by this gate. However, this crosstalk has a negative sign. In the coherent case, the total crosstalk is dominated by the beat terms (also with negative sign). The crosstalk of the gate only becomes important for very high input powers. In the incoherent case, the crosstalk is determined by the additive crosstalk of other channels in the absence of gate crosstalk (small input power, positive sign). When the input power is increased, the gate compensates for the additive crosstalk, resulting in a decrease of the total crosstalk. For a certain increase of input power the gate starts overcompensating and the total crosstalk changes sign from positive to negative see (6), the absolute value of the crosstalk, which is shown in the figure, then increases. The total crosstalk is dominated by the crosstalk of the gate. The place of the dip depends on the routing parameter and on the load. The place of the dip will change if partially zeros are transmitted.

The next figures are calculated in the case of coherent crosstalk.

2) *Crosstalk Parameter of the GC-SOA*: The influence of the crosstalk produced by the gate is only relevant for the topologies based on gates. The total crosstalk is calculated for topology 1 and 3.

The crosstalk is calculated for different values of the crosstalk parameter of the GC-SOA ( $X_{gate}$ ) (Fig. 12). The results are different for both OXC topologies. For the first OXC the crosstalk increases if the crosstalk of the gate increases.

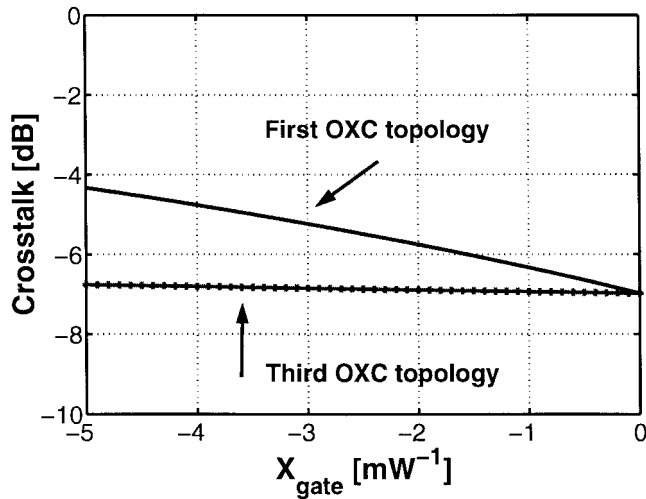


Fig. 12. Topology 1 and 3: Crosstalk (coherent) versus the crosstalk parameter of the GC-SOA. Full line is for the first topology and crossed line is for the third topology.

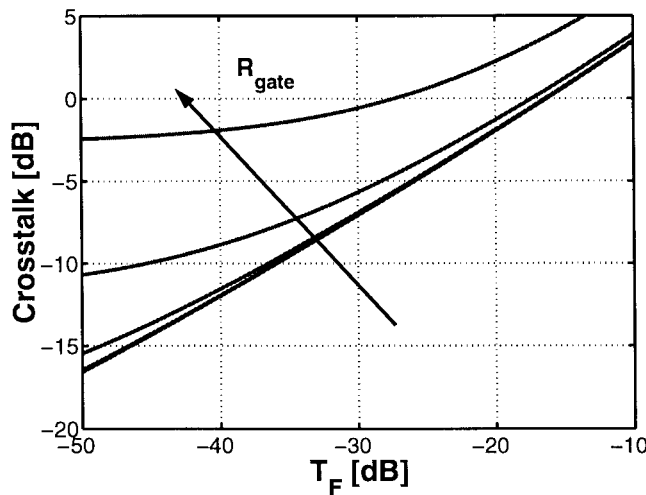


Fig. 13. Topology 1 and 3: Crosstalk (coherent) in function of the filter parameter for different on/off ratios ( $R = -10, -30, -50, -70$  and  $-90$  dB).

The third topology is much more robust against crosstalk of the gate, because the channels are filtered before being passed through the gates. This effect can be seen in the figure where the crosstalk for this topology is more or less independent of the crosstalk parameter of the gate. A realistic value of  $-0.1 mW^{-1}$  is used as bias value in the other calculations [47].

3) *Filter Parameter and ON-OFF Ratio:* The crosstalk is calculated in function of the filter parameter and the ON-OFF ratio of the gate for the first and the third topology. The results for both topologies are the same and are shown in Fig. 13. The total crosstalk in function of the filter parameter is shown for the ON-OFF ratio varied between 10 dB and 90 dB in steps of 20 dB. An ON-OFF ratio of 50 dB can be obtained with present gates, so one can conclude that higher ON-OFF ratios are not required. The total crosstalk is dominated by the filter. Better filters lead to better crosstalk performance [9], [25]. We can conclude that the filter limits the performance of the OXC in terms of total crosstalk.

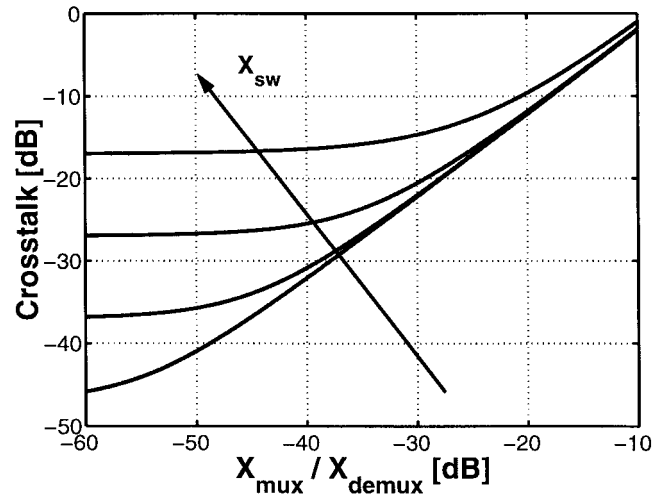


Fig. 14. Topology 2: Crosstalk (coherent) in function of the crosstalk of the Demultiplexer for different values of the Space Switch ( $X_{sw} = -40, -60, -80,$  and  $-100$  dB).

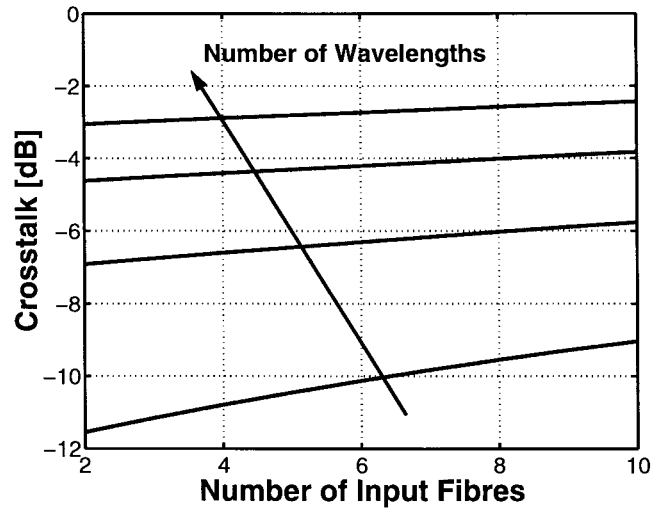


Fig. 15. Topology 1 and 3: Crosstalk (coherent) in function of the number of input fibers for different number of wavelength channels in a fiber ( $M = 2, 4, 6$  and  $8$ ).

4) *Crosstalk of the Space Switch and Demultiplexer:* The total crosstalk is calculated in function of the space switch and multiplexer/demultiplexer for the second topology (Fig. 14). The total crosstalk is dominated by the space switch as long as the crosstalk of the switch is smaller than twice the multiplexer-demultiplexer crosstalk. But mechano-optical space switches have very good crosstalk performances so in practise the total crosstalk will be limited by the crosstalk of the multiplexer/demultiplexer.

### C. Scalability of the OXC Topologies

To study the scalability of the OXC topologies the crosstalk (coherent) is calculated as a function of the number of input fibers  $N$  and the number of wavelengths in a fiber  $M$ . The results are presented in Figs. 15, 16, and 17 for the first/third, second and fourth topology. The results for the first and the third topology are as expected. The crosstalk strongly increases

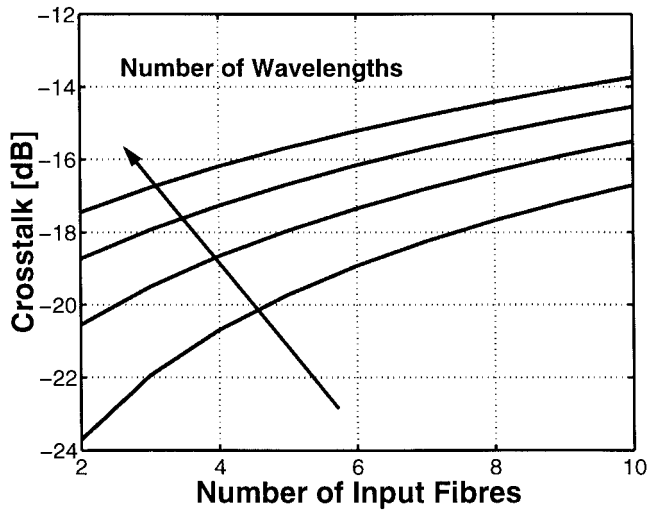


Fig. 16. Topology 2: Crosstalk (coherent) in function of the number of input fibers for different number of wavelength channels in a fiber ( $M = 2, 4, 6,$  and  $8$ ).

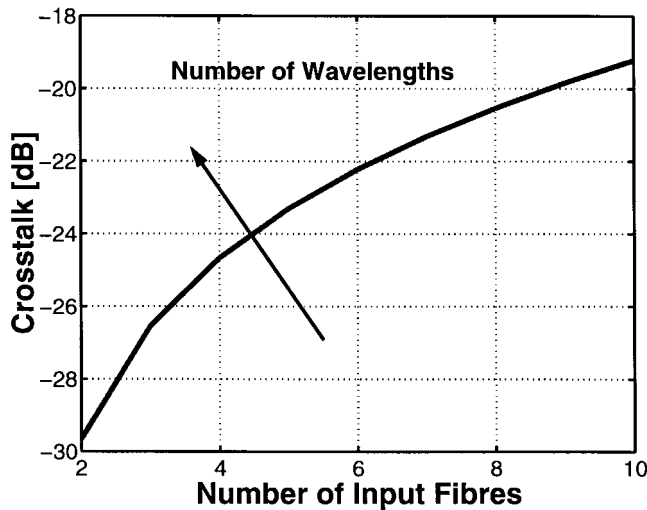


Fig. 17. Topology 4: Crosstalk (coherent) in function of the number of input fibers for different number of wavelength channels in a fiber ( $M = 2, 4, 6,$  and  $8$ ).

with  $N$  and  $M$ . For a certain throughput ( $N$  multiplied with  $M$ ) lowest crosstalk is obtained with large  $N$  and small  $M$ . If the total crosstalk will be kept constant and the number of fibers is increased ( $N$ ), the ON-OFF ratio ( $R_{gate}$ ) has to increase too. If the number of wavelengths is increased ( $M$ ), the filter suppression ( $T_F$ ) has to increase too.

The crosstalk of the second topology increases with increasing  $N$  and  $M$ . Optimal performance for a certain throughput ( $N \times M$ ) is obtained if the number of fibers equals the number of wavelengths ( $N = M$ ). If the total crosstalk is kept constant and the number of fibers increases ( $N$ ), the performance of the space switch ( $X_{switch}$ ) has to increase too. If the number of wavelengths is increased ( $M$ ), the multiplexer/demultiplexer suppression ( $X_{De-Mux}$ ) has to increase too.

The crosstalk of the fourth topology is almost independent of the number of wavelengths in a fiber ( $M$ ). This is due to the regeneration of the wavelength converter.

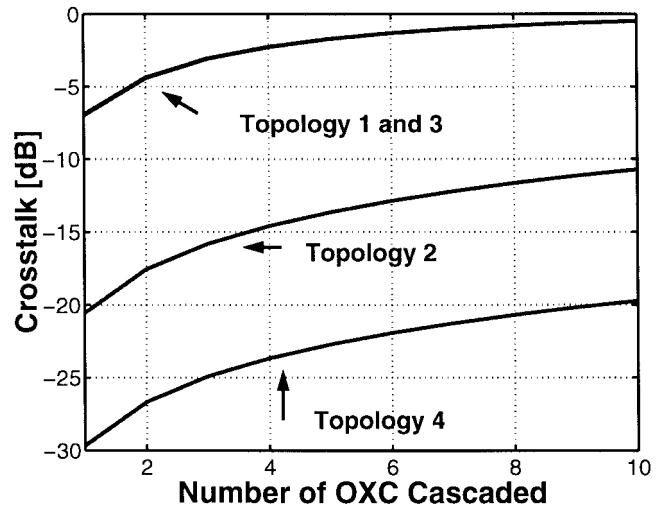


Fig. 18. Crosstalk (coherent) in function of the number of OXC's cascaded for four different topologies.

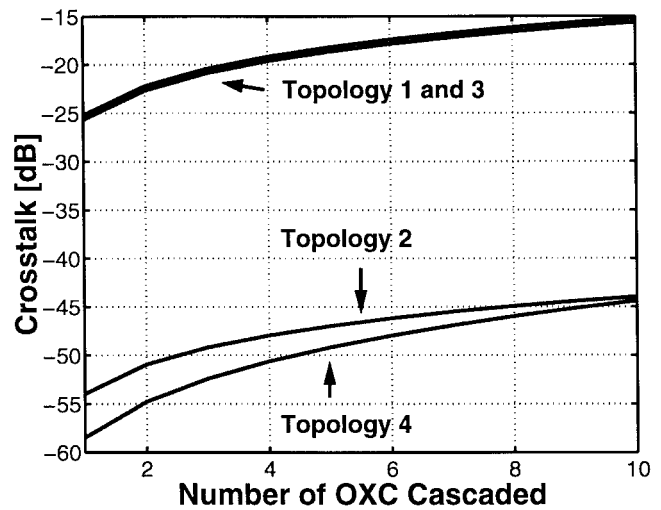


Fig. 19. Crosstalk (incoherent) in function of the number of OXC's cascaded for four different topologies.

In total one can conclude that the number of fibers can be increased without penalty if the performance of the switch is increased (gate or space switch). The number of wavelengths can be increased but requires higher suppression of other channels (filters or demultiplexers) or regeneration (wavelength converters). Realistic systems require a large number of wavelengths compared with the number of fibers. Therefore very good filters are required to reduce the crosstalk. If wavelength converters are used, the requirements for the filters are less strict.

#### D. Comparison of Different OXC Topologies in Terms of Crosstalk

In Fig. 18 the total crosstalk (coherent) is presented in function of the number of OXC cascaded and this for the four different topologies studied in this paper. As can be expected the highest crosstalk is obtained for the first and third topologies. Both topologies perform equally. The passive OXC based on the switch matrix performs much better. Best performance is obtained with the OXC including wavelength conversion.

The better performance of the passive topology compared to the first two topologies can be expected due to the low crosstalk values of the space switch, and because filtering occurs before and after the space switch.

The very good performance of the OXC with wavelength converters is due to the regeneration capabilities of the converter [49], [50] and due to the absence of interference crosstalk at the last combiner. If the crosstalk before the converter is small, it has little impact on the total crosstalk. The crosstalk before the converter can be reduced by optimising the crosstalk of the first topology. For that reason, the extensive study of the first topology is important. Optimal parameter settings for this topology will give optimal performance for the topology with wavelength converters. If the crosstalk before the wavelength converter is kept low, many converters can be cascaded.

From the comparison of the first and third topology, we conclude that they perform equally, independent of the place of the filter. The only difference is that the topology with selection before the switching, is not sensitive to variations in the crosstalk parameter of the gate, while the first topology with the selection after the switch matrix is very sensitive.

By comparing the first two topologies, we see that the first one has considerable higher crosstalk. But this topology contains only one filter and the second topology contains two filters, one in front of and one behind the switch. From the calculations in function of the component parameters we see that both topologies are limited by the filter. We can conclude that the mechano-optical space switch performs better than the switch based on gates (even better performance is mentioned in literature [9], but in both cases the total crosstalk is limited by other components.

The wavelength converter improves the performance of an OXC topology drastically (comparison between the first and the last OXC). The drawback is that converters are very expensive and that they add jitter.

Optimal crosstalk performance will be obtained if filtering before and after the switch matrix is accomplished and wavelength conversion is used. Both switch matrixes perform good. The crosstalk of the switch is not dominant as long as it is better than twice the filter suppression. If gates are used in the switch matrix, the total input power should be sufficiently low so that the gain of the gate is clamped. This can be obtained by filtering in front of the switch.

The incoherent crosstalk in function of the number of OXC cascaded is shown in Fig. 19 (The crosstalk of topology 1 is calculated with an input power of  $-30$  dBm to avoid dominant gate crosstalk). While the coherent crosstalk gives an upper limit, the incoherent crosstalk gives a lower limit which can be obtained with a certain set of component parameters. The margin between upper and lower limit indicates the improvement which can be obtained by suppressing the beat term. This can be obtained for example by phase scrambling. If a crosstalk value of  $-20$  dB can be tolerated, only the OXC with wavelength converters satisfies the demand if a number of cross connects is cascaded. By suppressing the beat term the same tolerance can be fulfilled with the second topology.

One can conclude that a calculation in the case of coherent crosstalk gives an upper boundary. When this upper boundary

does not meet the requirements there is room for improvement by suppressing the beat. An incoherent calculation results in a lower boundary. If this lower boundary is not good enough, better component parameters are required.

## VI. CONCLUSION

In this paper, four different OXC topologies have been studied. Their crosstalk sources have been identified and their total crosstalk is calculated based on analytical equations. Good qualitative agreement with the numerical simulations have been demonstrated.

From the comparison between the different OXC's we can conclude that the performance is limited by the filters. Both switch matrixes fulfill the demand. Wavelength converters improve the system and make the filter requirements less strict. That is why they could be necessary in future optical cross connects. A high input power of the gates will result in an extra penalty. Optimal results are obtained if filters are used in front of and behind the switch and if wavelength converters are applied.

A big difference between coherent crosstalk and noncoherent crosstalk has been observed as was expected. To reduce the coherent crosstalk, phase scramblers could be used. A calculation in case of coherent crosstalk gives an upper boundary on the expected crosstalk, a calculation of the incoherent case results in a lower boundary. If the lower boundary does not meet the requirements better components are necessary.

## REFERENCES

- [1] C. A. Brackett, "Is there an emerging consensus on WDM networking," *J. Lightwave Technol.*, vol. 14, pp. 936-941, June 1996.
- [2] D. J. Blumenthal, M. Shell, and M. D. Vaughn, "Physical limitations to scalability of WDM all-optical networks," *Opt. Photon. News*, Feb. 1997.
- [3] V. Mizrahi *et al.*, "The future of WDM systems," in *Proc. ECOC 1997*, 1997, pp. 137-141.
- [4] M. Artiglia, "Upgrading installed systems to multigigabit bit-rates by means of dispersion compensating," in *Proc. ECOC 1996*, MoB4, pp. 1.75-1.82, 1996.
- [5] M. J. O'Mahony, "Results from the COST 239 project: Ultra-high capacity optical transmission networks," in *Proc. ECOC 1996*, TuB1.2, pp. 2.11-2.18, 1996.
- [6] H. Kogelnik, "WDM networks: A U.S. perspective," in *Proc. ECOC 1996*, MoA 2.2, pp. 5.81-5.86, 1996.
- [7] M. J. O'Mahony, D. Simeonidou, A. Yu, J. Zhou, "The design of a european optical network," *J. Lightwave Technol.*, vol. 13, pp. 817-828, May 1995.
- [8] G. R. Hill *et al.*, "A transport network layer based on optical network elements," *J. Lightwave Technol.*, vol. 11, pp. 667-679, May/June 1993.
- [9] M. Erman, "What technology is required for the pan-european network, what is available and what is not," in *Proc. ECOC 1996*, TuB 2.2, pp. 5.87-5.94, 1996.
- [10] A. Jourdan, F. Masetti, M. Garnot, G. Soulage, and M. Sotom, "Designs and implementation of a fully reconfigurable all-optical crossconnect for high capacity multiwavelength transport networks," *J. Lightwave Technol.*, vol. 14, pp. 1198-1206, June 1996.
- [11] A. Jourdan *et al.*, "Fully reconfigurable WDM optical crossconnect: Feasibility validation and preparation of prototype crossconnect for ACTS 'OPEN' field trials," in *Proc. ECOC 1997*, pp. 55-58, 1997.
- [12] M. W. Chbat *et al.*, "The OPEN ACTS project: Early achievements and perspectives," in *Proc. ECOC 1996*, WeP 1.1, pp. 3.253-3.256.
- [13] A. Jourdan *et al.*, "WDM networking experiment including all-optical crossconnect cascade and transmission over 320 km G.652 fiber to 10 Gbit/s," in *Proc. ECOC 1996*, ThD 1.6, pp. 4.123-4.126.
- [14] D. Chiaroni *et al.*, "Feasibility issues of a high-speed photonic packet switching fabric based on WDM subnanosecond optical gates," in *Proc. ECOC 1996*, ThD. 1.7, pp. 4.127-4.130.

- [15] C. A. Brackett, "Dense wavelength division multiplexing networks: Principle and applications," *J. Select. Areas Commun.*, vol. 8, pp. 948–964, Aug. 1990.
- [16] B. Mikkelsen, K. Wunsel, P. Doussiere *et al.*, "Demonstration of a robust WDM cross-connect cascade based on all-optical wavelength converters for routing and wavelength slot interchange," in *Proc. ECOC 1997*, pp. 245–248.
- [17] R. E. Wagner *et al.*, "Realising the vision of multiwavelength optical networking," in *Proc. ECOC 1997*, pp. 143–147.
- [18] P. B. Hansen, M. Shilling, P. Doussiere *et al.*, "20 Gbit/s experimental demonstration of all-optical WDM packet switch," in *Proc. ECOC 1997*, pp. 13–16.
- [19] M. Teshima *et al.*, "Demonstration of virtual wavelength path cross-connect," in *Proc. ECOC 1997*, pp. 59–62.
- [20] M. Rasztovits-Wiech *et al.*, "PHOTON—A progressive step toward optical transport networks in europe," in *Proc. NOC'96*, vol. 1, pp. 174–181.
- [21] O. Ishida, N. Takachio, and K. Sato, "Modular cross-connect system for WDM optical-path networks," in *Proc. ECOC 1997*, pp. 63–66.
- [22] C. Casper, H. M. Foisel, E. Patzak, B. Strebel, and K. Weich, "Improvement of crosstalk tolerance in optical cross connects by regenerative frequency converters," in *Proc. ECOC 1996*, ThD 1.5, pp. 4.119–4.122.
- [23] H. Takahashi *et al.*, "Impact of crosstalk in an arrayed-waveguide multiplexer on  $N \times N$  optical interconnection," *J. Lightwave Technol.*, vol. 14, pp. 1097–1105, June 1996.
- [24] G. Eilenberger *et al.*, "Cascadability of transparent WDM routing nodes using regenerating wavelength conversion components," in *Proc. ECOC 1996*, MoA 4.4, pp. 1.35–1.38.
- [25] G. Soulage *et al.*, "4 × 4 space-switch based on clamped-gain semiconductor optical amplifiers in a 16 × 10 Gbit/s WDM experiment," in *Proc. ECOC 1996*, ThD 2.1, pp. 4.145–4.148.
- [26] C. Li and F. Tong, "Crosstalk and interference penalty in all-optical networks using static wavelength routers," *J. Lightwave Technol.*, vol. 14, pp. 1120–1126, June 1996.
- [27] J. Zhou *et al.*, "Crosstalk in multiwavelength optical cross connect networks," *J. Lightwave Technol.*, vol. 14, pp. 1423–1435, June 1996.
- [28] H. Sano, Y. Sawada *et al.*, "Novel optical cross-connect architecture for restoration in backbone networks," in *Proc. ECIO 1997*, PThA5, pp. 84–87.
- [29] R. T. Hofmeister *et al.*, "Project Learn—Light exchanegable, add/drop ring network," in *Proc. OFC 1997*, PD25, 1997.
- [30] R. S. Vodhanel *et al.*, "National-scale WDM networking demonstration by the MONET consortium," in *Proc. OFC 1997*, PD27.
- [31] H. Obara and T. Kawai, "Virtually crosstalk-free wavelength routing network architecture," *Electron. Lett.*, vol. 32, no. 6, pp. 1123–1125, June 1996.
- [32] M. F. Stephens, M. J. O'Mahony, M. J. Robertson *et al.*, "Demonstration of a flexible all-optical wavelength converting/routing switch architecture," in *Proc. ECOC 1996*, ThD 1.9, pp. 4.135–4.138.
- [33] M. Koga *et al.*, "Optical path cross-connect demonstrator designed to achieve 320 Gbit/s," in *Proc. ECOC 1996*, ThC 3.1, pp. 5.29–5.32.
- [34] M. Koga *et al.*, "Design and performance of an optical path cross-connect system based on wavelength path concept," *J. Lightwave Technol.*, vol. 14, pp. 1106–1119, June 1996.
- [35] Y. Jin and M. Kavehrad, "An optical cross-connect system as a high-speed switching core and its performance analysis," *J. Lightwave Technol.*, vol. 14, pp. 1183–1197, June 1996.
- [36] R. E. Wagner *et al.*, "MONET: Multiwavelength optical networking," *J. Lightwave Technol.*, vol. 14, pp. 1349–1355, 1996.
- [37] A. M. Hill and D. B. Payne, "Linear crosstalk in wavelength-division-multiplexed optical fiber transmission systems," *J. Lightwave Technol.*, vol. LT-3, pp. 643–650, June 1985.
- [38] C. P. Larsen, L. Gillner and M. Gustavsson, "Linear crosstalk properties of large WDM cross-connects," in *Proc. ECIO 1997*, PWA4, pp. 27–30.
- [39] D. J. Blumenthal, "Coherent crosstalk in photonic switched networks," in *Proc. ECIO 1997*, PWA1, pp. 1–6.
- [40] L. Gillner, C. P. Larsen, and M. Gustavson, "Influence of crosstalk on the scalability of optical multi-wavelength switching networks," in *Proc. LEOS Summer Topical Meeting*, Montreal, P.Q., Canada, Aug. 1997, TuC2, pp. 32–33.
- [41] G. A. Castanon, O. K. Tonguz, and A. Bononi, "Impact of crosstalk on the performance of multi-wavelength optical cross-connected networks using deflection routing," in *Proc. LEOS 1996*, ThG4, pp. 318–319.
- [42] Y. K. Park *et al.*, "Crosstalk and prefiltering in a two-channel ASK heterodyne detection system without the effect of laser phase noise," *J. Lightwave Technol.*, vol. 6, pp. 1312–1319, Aug. 1988.
- [43] D. J. Blumenthal, P. Grandstrand, and L. Thylen, "BER floors due to heterodyne coherent crosstalk in space photonic switches for WDM networks," *IEEE Photon. Technol. Lett.*, vol. 8, pp. 284–286, Feb. 1996.
- [44] O. Lindunger and E. Almstrom, "Time dependence of interferometric crosstalk in all-optical networks," in *Proc. ECIO 1997*, PWA3, pp. 23–26.
- [45] P. B. Hansen and L. Eskildsen, "Multi-path interference in optically pre-amplified lightwave systems," in *Proc. ECOC 1997*, pp. 271–274.
- [46] P. Ohlen and E. Berglund, "Noise accumulation and BER estimates in concatenated nonlinear optoelectronic repeaters," *IEEE Photon. Technol. Lett.*, vol. 9, pp. 1011–1013, July 1997.
- [47] J. Sun, G. Morthier, and R. Baets, "Numerical and theoretical study of the crosstalk in gain clamped semiconductor optical amplifiers," *IEEE J. Select. Topics Quantum Electron.*, vol. 3, pp. 1162–1167, Oct. 1997.
- [48] T. Durhuus *et al.*, "Detailed dynamic model for semiconductor optical amplifiers and their crosstalk and intermodulation distortion," *J. Lightwave Technol.*, vol. 10, pp. 1056–1065, Aug. 1992.
- [49] B. Mikkelsen *et al.*, "All-optical noise reduction capability of interferometric wavelength converters," *Electron. Lett.*, vol. 32, no. 6, pp. 566–567, 1996.
- [50] T. Gyselings, G. Morthier and R. Baets, "Strong improvement in optical signal regeneration and noise reduction through asymmetric biasing of mach-zehnder interferometric all-optical wavelength converters," in *Proc. ECOC 1997*, pp. 188–191.
- [51] T. Durhuus *et al.*, "All-optical wavelength conversion by semiconductor optical amplifiers," *J. Lightwave Technol.*, vol. 14, pp. 942–954, June 1996.
- [52] K. Vreeburg, "InP-based photonic integrated circuits for wavelength routing and switching," Ph.D. dissertation, Univ. Delft, The Netherlands, Dec. 1997, ch. 5.
- [53] W. V. Parys, B. Van Caenegem, and B. Vandenberghe, "Meshed wavelength-division multiplexed networks partially equipped with wavelength converters," in *Proc. OFC 1998*, ThU1, pp. 359–360.
- [54] K. Okamoto, "Integrated optical WDM devices," in *Proc. ECIO 1997*, EWC1, pp. 62–67.

**Tim Gyselings** (S'98) was born in Deurne, Belgium, on February 19, 1972. He received the degree in electrical engineering from the University of Gent, Belgium, in 1995.

Since 1995, he has been with the Department of Information Technology (INTEC) of the University of Gent. He holds a research fellowship at the Flemish Institute for Science and Technology (IWT). His main interests are the modeling of WDM networks.

Mr. Gyselings is a student member of IEEE Laser and Opto-Electronics Society (LEOS), IEEE Communications Society (COMSOC), and the Flemish Engineer Association.

**Geert Morthier** (M'88) was born in Gent, Belgium, on March 20, 1964. He received the degree in electrical engineering and the Ph.D. degree from the University of Gent in 1987 and 1991, respectively.

Since 1991, he has been a member of the permanent staff of the IMEC at the University of Gent. His main interests are in the modeling and characterization of optoelectronic components. He has authored or coauthored over 70 papers in the field. He is also one of two authors of the *Handbook of Distributed Feedback Laser* (Norwood, MA: Artech House, 1997) and coeditor of the book *How to Model and Measure Photonic Components: Experience From a European Project* (New York: Springer-Verlag, 1998).

Dr. Morthier is a member of the Optical Society of America (OSA).

**Roel Baets** (M'88–SM'96) received the degree in electrical engineering from the University of Gent, Gent, Belgium, in 1980. He received the M.Sc. degree in electrical engineering from Stanford University, Stanford, CA, in 1981 and the Ph.D. degree from the University of Gent in 1984.

Since 1981, he has been with the Department of Information Technology (INTEC) of the University of Gent. Since 1989, he has been a Professor in the Engineering Faculty of the University of Gent. From 1990 to 1994, he has also been a part-time Professor at the Technical University of Delft, Delft, The Netherlands. He has worked in the field of III–V devices for optoelectronic systems. With over 100 publications and conference papers, he has made contributions to the modeling of semiconductor laser diodes, passive guided-wave devices, and to the design and fabrication of OEIC's. His main interests now are the modeling, design and testing of optoelectronic devices, circuits and systems for optical communication, and optical interconnect.

Dr. Baets is a member of the IEEE Laser and Opto-Electronics Society, SPIE, Optical Society of the America (OSA), and the Flemish Engineer Association. He has been member of the program committees of OFC, ECOC, IEEE Semiconductor Laser Conference, ESSDERC, CLEO-Europe and the European Conference on Integrated Optics.